

# The effect of phloretin on single potassium channels in myelinated nerve

J. Klusemann and H. Meves

I. Physiologisches Institut der Universität des Saarlandes, W-6650 Homburg-Saar, Federal Republic of Germany

Received January 31, 1992/Accepted in revised form March 18, 1992

**Abstract.** The effect of phloretin, a dipolar organic compound, on single potassium channel currents of myelinated nerve fibres of *Xenopus laevis* has been investigated, using inside-out patches prepared by the method of Jonas et al. (1989). The *I* channel, a potential dependent K channel with intermediate deactivation kinetics, was reversibly blocked by 20  $\mu$ M phloretin applied on the inside; the block was strongest at negative membrane potentials and less pronounced at positive potentials. Phloretin shifted the curve relating open probability to membrane potential towards more positive potentials and reduced its slope and maximum. This confirms previous findings on the effect of phloretin on the voltage dependence of the fast macroscopic K conductance. Single channel conductance and deactivation kinetics were not altered by phloretin.

**Key words:** Nerve fibre – Potassium channel – Phloretin

## Introduction

Phloretin in micromolar concentrations has a marked effect on the K channels of squid giant axons (Strichartz et al. 1980; Spiro and Begenisich 1989): it reduces the K conductance  $g_K$ , shifts the voltage dependence of  $g_K$  to more positive potentials, decreases its slope and slows the rise of the K current  $I_K$ . The same is seen in the frog node of Ranvier (Klusemann and Meves 1991). However, of the three classes of K channels that exist in this preparation (fast 1, fast 2 and slow, see Dubois 1981) only the components fast 1 and fast 2, not the slow component, are affected by phloretin.

Jonas et al. (1989) succeeded in recording single channel currents from Na and K channels in the nodal and paranodal membrane of myelinated nerve fibres from *Xenopus laevis*. They found three types of K channels, called *F* (fast), *I* (intermediate), *S* (slow) according to their

deactivation kinetics. The *I* channel is the most frequent type. It deactivates more slowly than the macroscopic component fast 1 but resembles the latter in two respects: it activates between  $-60$  and  $-30$  mV, in a similar way to fast 1, and is blocked by dendrotoxin, a specific blocker of fast 1.

The present paper reports that phloretin affects single *I* channels in the same way as it affects the fast component of the macroscopic K current, lending further support to the notion that *I* channels correspond to the fast component of the macroscopic  $I_K$ .

Part of the results have been published in abstract form (Klusemann and Koh 1991; Klusemann and Meves 1992).

## Methods

Fibres of the sciatic nerve of *Xenopus laevis* were demyelinated and patch-clamped according to the method of Jonas et al. (1989), modified by Jonas et al. (1991). Briefly, the nerve was treated with collagenase, subsequently incubated in Ca-free Ringer solution with protease, cut into segments of 0.5–1 mm length and dissociated into single fibres by gently shaking. Measurements were made on inside-out patches at 15°C. Pipettes had resistances of 20–25 M $\Omega$  and were coated with Sylgard and fire-polished. Currents were elicited by voltage pulses and measured with a List EPC-7 amplifier. A DEC PDP 11/23 microcomputer generated the voltage pulses, collected the data at a 10 kHz sampling rate (after low-pass filtering with a cut-off frequency of 1 kHz) and was used for off-line analyses.

## Solutions

The Ringer solution contained 110 mM NaCl, 2.5 mM KCl, 2 mM CaCl<sub>2</sub> and the Ca<sup>2+</sup>-free Ringer 110 mM NaCl, 2.5 mM KCl, 3 mM EGTA. The experiments were done with 105 mM KCl, 13 mM NaCl, 3 mM EGTA in the bath

(i.e. on the intracellular side of the membrane) and 105 mM KCl, 13 mM NaCl, 2 mM  $\text{CaCl}_2$  in the pipette (i.e. on the extracellular side). 300 nM tetrodotoxin was added to the pipette solution to block the Na channels. All solutions were buffered with 5 mM BES(N,N-bis-(2-hydroxyethyl)-2-aminoethane sulfonic acid) at pH 7.2–7.4. From a stock solution of 20 mM phloretin in dimethylsulfoxide (DMSO) an appropriate amount was added to the bath solution (final DMSO concentration <0.2%). A multi-barrel perfusion system was used to change quickly from phloretin-free to phloretin-containing bath solution.

### Analysis

Current amplitude histograms were constructed and fitted with Gaussian curves. From the integrals of the Gaussian curves the product  $NP_0$  (where  $N$  is the number of channels in the patch and  $P_0$  the probability of a channel being open) was obtained.  $NP_0(E)$  was calculated as

$$NP_0 = F1 + 2F2 + 3F3$$

where  $F1$ ,  $F2$ ,  $F3$  denote the area under the Gaussian curve for one, two or three channel openings, respectively (for details, see Gola et al. 1990). The formula  $P_0 = (F1/F_C)/(N + F1/F_C)$ , derived for a binomial distribution with  $F_C$  being the area under the Gaussian curve for the closed state, gave very similar results.  $NP_0(E)$  was fitted by a Boltzmann equation

$$NP_0 = (NP_0)_{\max} / [1 + \exp((E_{\text{mid}} - E)/k)] \quad (1)$$

where  $E_{\text{mid}}$  is the potential at which  $NP_0$  reaches half of its maximum  $(NP_0)_{\max}$  and  $k$  is a reciprocal slope factor in mV per  $e$ -fold change. Fitting routines were based on the least-squares algorithm.

### Sign convention

Membrane potentials are given using the usual convention of the extracellular surface being the reference or ground. Inward currents are shown as downward deflections.

## Results

### Multichannel patches

It was easy to obtain patches with a relatively large number of channels. Experiments with such patches confirmed the results obtained with macroscopic tail currents. With 105 mM KCl on both sides of the membrane, a 50 ms pulse from  $-80$  to  $-40$  mV elicited a brief capacity transient and a more slowly rising inward current which, upon repolarization, was followed by another capacity transient and a long-lasting inward tail current (Fig. 1A). The initial amplitude of the tail current was about twice as large as the inward current flowing immediately before the end of the pulse; this is expected be-

cause the driving force is twice as large. The tail current in its later part decayed in a stepwise fashion, reflecting the closing of individual channels. Application of  $40 \mu\text{M}$  phloretin almost totally suppressed the inward current during the pulse and the inward tail current after the pulse (Fig. 1B). They returned after a 3 min wash with phloretin-free solution (Fig. 1C). The measurements were repeated with other pulse potentials, ranging from  $-60$  to  $80$  mV.

For a quantitative analysis, the tail current was integrated from 0 to 175 ms after the end of the pulse and the integral, charge  $Q$  in pC, plotted against pulse potential  $E$  (Fig. 2). The resulting sigmoid curves describe the potential-dependent activation of the channels in the patch. They show that  $40 \mu\text{M}$  phloretin reversibly reduces the slope of the curve and shifts its midpoint potential  $E_{\text{mid}}$  to much more positive potentials, resembling its effect on the  $g_K(E)$  curve of the fast component of the macroscopic  $I_K$ . The phloretin effect was reversible.  $Q_{\max}$  was even somewhat larger after wash than in control (see legend of Fig. 2), probably owing to the slower deactivation kinetics after wash (compare records A and C in Fig. 1).

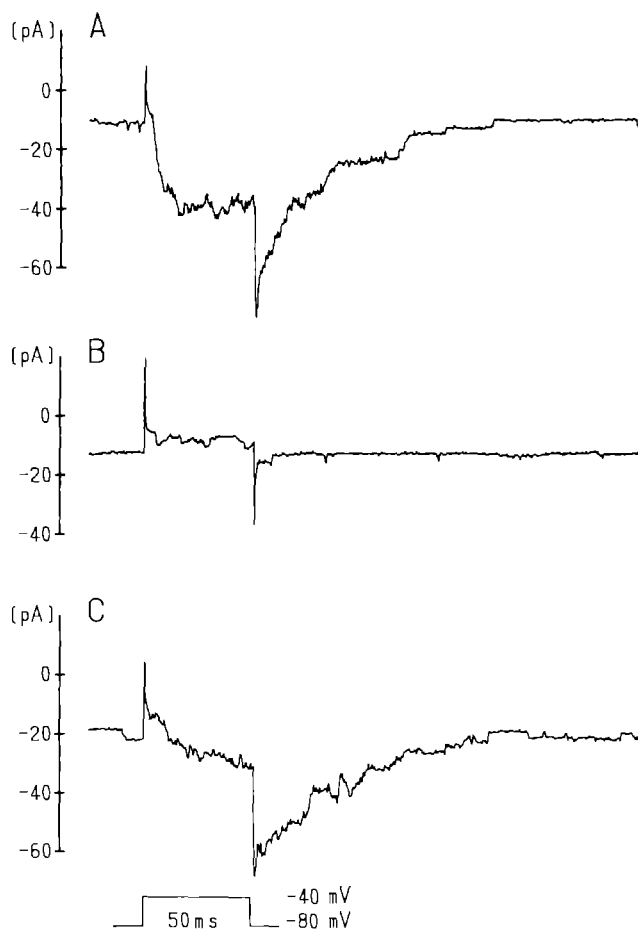


**Fig. 1** A–C. Effect of  $40 \mu\text{M}$  phloretin on a multichannel patch. **A** control, **B**  $40 \mu\text{M}$  phloretin in bath for 3 min. **C** after washing with phloretin-free solution for 3 min. Holding potential  $-80$  mV. The holding current increased during the experiment from  $-11$  to  $-19$  pA. The records show the current before, during and after a 50 ms pulse to  $-40$  mV

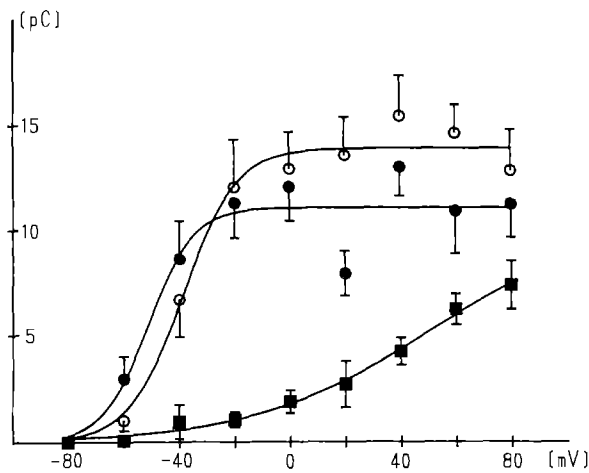


**Fig. 2.** Tail current integral plotted against pulse potential for control (●), 40  $\mu$ M phloretin (■) and wash (○). Same experiment as in Fig. 1. Points are means  $\pm$  SEM from 11 measurements. Tail currents were integrated from 0 to 175 ms after the end of the pulse. Points ● and ○ were fitted by

$$Q = Q_{\max} / [1 + \exp((E_{\text{mid}} - E)/k)] \quad [\text{fC}]$$

with the following parameters:

	$Q_{\max}$	$E_{\text{mid}}$	$k$
Control	-11.1 pC	-51.1 mV	8.2 mV
Wash	-14.0 pC	-38.5 mV	9.7 mV

The curve through points ■ was drawn by eye

### Patches with a few *I* channels

Tail events from a patch containing only four channels are illustrated in Fig. 3 and the corresponding amplitude histograms are shown in Fig. 4. Under control conditions (left vertical row) pulses to -40, 40 or 80 mV are followed by tail events of 2.1–2.2 or 4.4–4.8 pA amplitude. These are currents through one or two K channels which have been opened by the 50 ms pulse and stay open for some time after the pulse end. Channel reopenings are also visible (records G and I). Dividing the single channel currents by the driving force (-80 mV) gives an average single channel chord conductance of 27.9 pS, similar to the average single channel conductances of Jonas et al. (1989) for I channels (23 pS) and F channels (30 pS). Calculating the relative open probability  $NP_0$  from the amplitude histograms yields a  $NP_0(E)$  curve which rises steeply between -60 and -40 mV (Fig. 5, symbols ○). According to Jonas et al. (1989) the steep rise is typical for I channels, not for the less frequent F channels. We therefore conclude that the channels in Figs. 3–5 are I channels.

For a quantitative analysis, points ○ in Fig. 5 have been fitted with a Boltzmann equation. The parameters in the legend of Fig. 5 are similar to those given for I channels by Jonas et al. (1989) in the legend of their Fig. 5C ( $E_{\text{mid}} = -35$  mV,  $k = 3.8$  mV), but  $E_{\text{mid}}$  is 14 mV more negative in our experiment. In another experiment we found  $E_{\text{mid}} = -56$  mV. It should be noted that Fig. 5C of Jonas et al. (1989) is from an axon-attached patch whereas our measurements were done on inside-out patches. In the latter, the voltage dependence of excitability param-

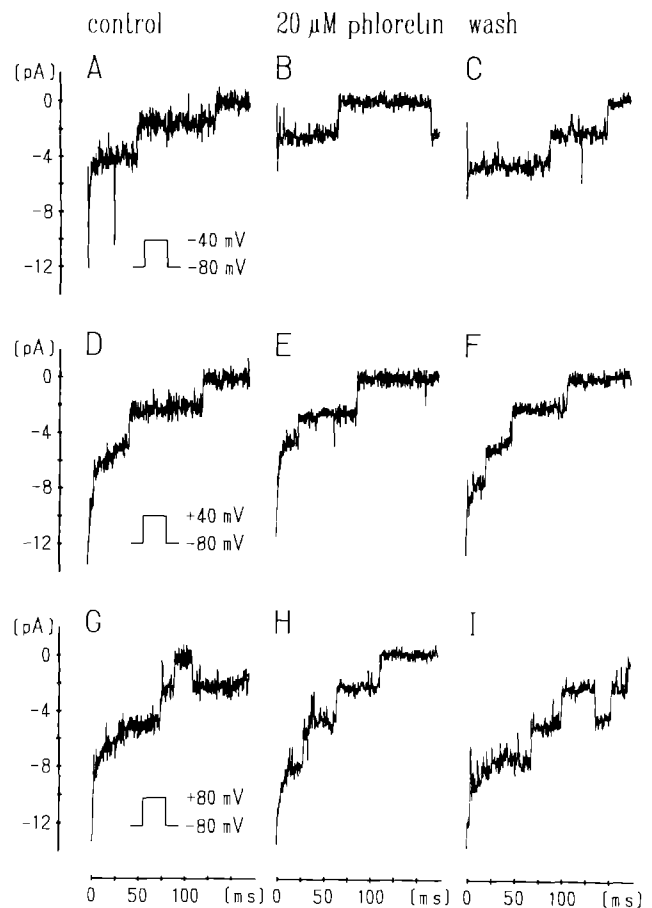


**Fig. 3.** Single channel records from a patch in which up to four channels are simultaneously open. *Left row*, control. *Middle row*, 20  $\mu$ M phloretin in bath for 4 min. *Right row*, after washing with phloretin-free solution for 3 min. The records show tail events at a holding potential of -80 mV following 50 ms pulses to -40 mV (*upper row*), +40 mV (*middle row*) or +80 mV (*lower row*). Repolarization to the holding potential occurs at 0 ms. The capacitive current at the pulse end is visible as a brief surge of inward current. Holding current subtracted.  $i = 0$  denotes the closed channel state

ters is usually shifted to more negative potential values in comparison with cell-attached patches (Fenwick et al. 1982; Nagy et al. 1983).

The effect of 20  $\mu$ M phloretin can be clearly seen in the amplitude histograms of Fig. 4. At -40 mV (Fig. 4A–C) phloretin markedly increased the occurrence of the closed state ( $i = 0$  pA). Single channel openings were rarer than in control, double openings were very rare. The effect of phloretin was reversible. At more positive potentials (Fig. 4D–I) the blocking effect of phloretin was less pronounced. But even at 40 and 80 mV the closed state ( $i = 0$  pA) was more frequent in phloretin than in control or after wash. The  $NP_0(E)$  curve in Fig. 5 is altered accordingly: its maximum and its slope are reduced, its midpoint potential is shifted to more positive potentials, similar to the phloretin effect on the fast component of the macroscopic  $I_K$ . Phloretin did not alter the single channel conductance as can be seen from the current peaks in Fig. 4.

In Fig. 5, 20  $\mu$ M phloretin blocked 82% of the tail events following pulses to -40 mV. With 5 or 10  $\mu$ M

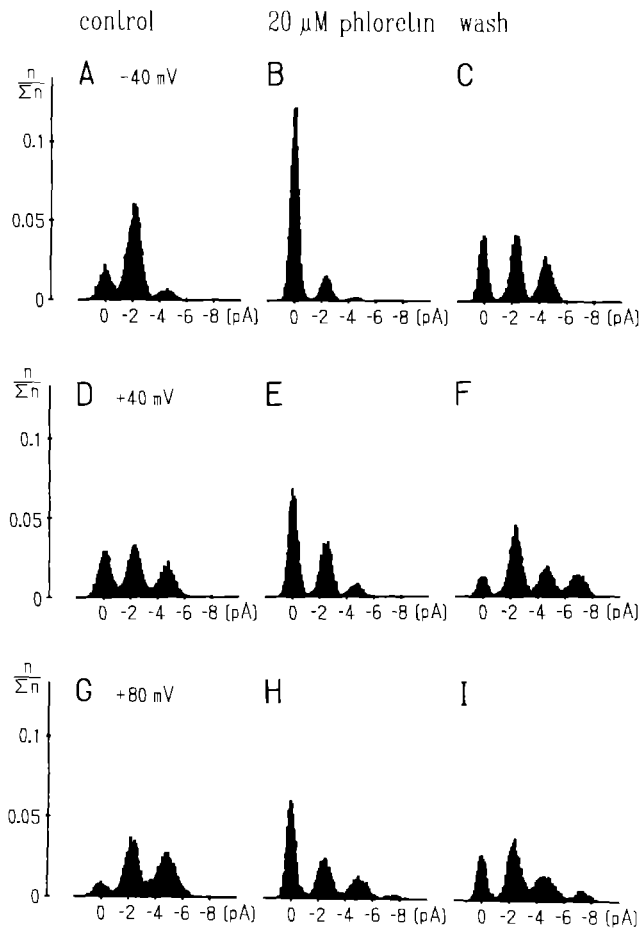


**Fig. 4.** Current amplitude histograms for tail events following pulses to  $-40$ ,  $40$  and  $80$  mV in control,  $20 \mu\text{M}$  phloretin and wash. Same experiment as Fig. 3. Each histogram is based on 14–17 records. The first 170 ms after repolarisation to the holding potential were used for the analysis. Plotted are the relative numbers  $n/\Sigma n$  of sampled current values in bins of  $0.1$  pA width (total number of values  $\Sigma n = 8414$ – $10217$ )

phloretin the blocking effect was smaller but still visible. This can be seen in Fig. 6 which shows a dose-response curve for phloretin based on four experiments. It yields a half blocking concentration of  $7.0 \mu\text{M}$ .

Klusemann and Meves (1991) emphasized that phloretin does not affect the time constant of the fast component of the macroscopic tail current. Figure 7 shows open time histograms for tail events following pulses to  $40$  and  $80$  mV in control and phloretin. If the rare reopenings (see records G and I in Fig. 3) are neglected, these histograms correspond to the conditional open-time histograms of Nagy (1987). They give the probability of finding a channel open, provided it was open at the pulse end. The histograms in Fig. 7 were fitted with the sum of two exponential functions. The first component probably reflects the fast flickering in the original records (see Fig. 3). The time constant of the second exponential function is presumably determined by the open  $\rightarrow$  close transition rate of the channels in the patch. It is not significantly affected by phloretin.

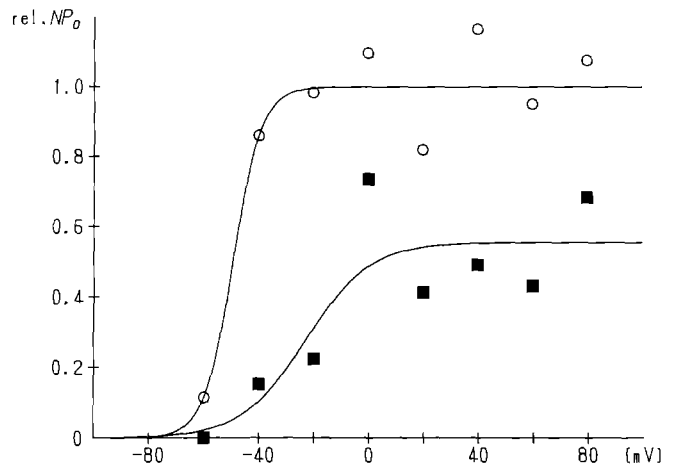


**Fig. 5.** Relative open probability  $NP_0$  as function of membrane potential for  $20 \mu\text{M}$  phloretin ( $\blacksquare$ ) and control ( $\circ$ ). The control measurements shown were done *after* phloretin. Same experiment as Figs. 3–4. Measurements at  $60$  and  $80$  mV in control gave an average of  $1.26$ . This was taken as  $NP_0 = 1$  and all other  $NP_0$  values were normalized to  $1.26$ . Points were fitted by Eq. (1) with the parameters

	Phloretin	Control
$(NP_0)_{\max}$	$0.55$	$1.0$
$E_{\text{mid}}$	$-23$ mV	$-49$ mV
$k$	$11.8$ mV	$5.2$ mV

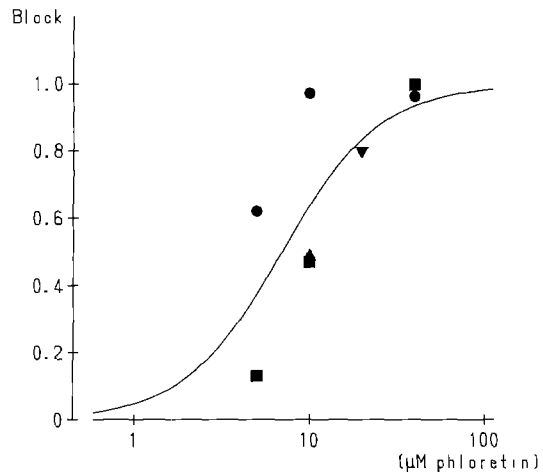


**Fig. 6.** Dose-response curve for the blocking effect of phloretin on tail events following pulses to  $-40$  mV. Ordinate:  $\text{block} = 1 - (NP_0 \text{ in phloretin}) / (NP_0 \text{ in control})$ . Abscissa: phloretin concentration  $C$  on a logarithmic scale. The symbols refer to four different experiments,  $\blacktriangledown$  to the experiment of Figs. 3–5. The points are fitted by the equation

$$\text{block} = [1 + (IC_{50}/C)^a]^{-1}$$

with  $IC_{50} = 7.0 \mu\text{M}$  and a Hill coefficient  $a = 1.55$

## Discussion

The single channel experiments confirm our previous findings about the effect of phloretin on the macroscopic K current. Phloretin has the same effect on the  $P_0(E)$  curve of single I channels as it has on the  $g_K(E)$  curve of the fast component of the macroscopic  $I_K$ . Both curves are shifted to more positive potentials; their slope and

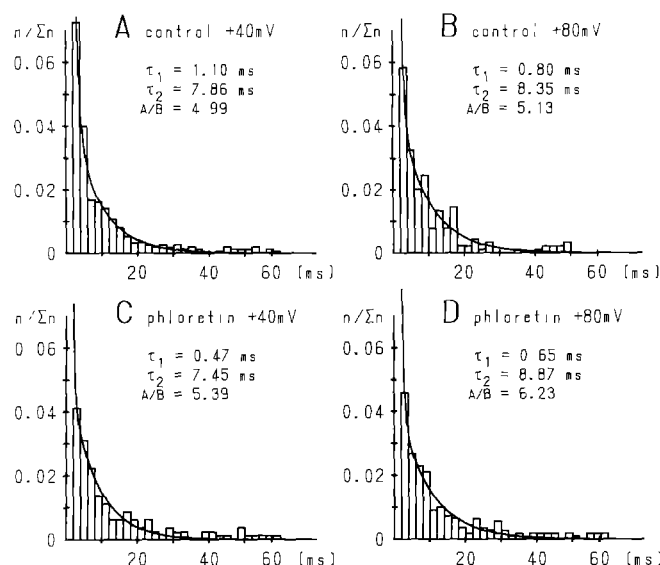


**Fig. 7.** Open time histograms for tail events following pulses to 40 and 80 mV in control (A, B) and 20  $\mu$ M phloretin (C, D). Same experiment as Figs. 3–5. The curves represent fits with the equation  $y = A \exp(-t/\tau_1) + B \exp(-t/\tau_2)$ . The time constants  $\tau_1$  and  $\tau_2$  and the ratios  $A/B$  are indicated. Bin width 2 ms

their maximum are reduced. Neither the time course of the macroscopic fast tail current nor the deactivation kinetics of the I channels are affected by phloretin. It should be noted that phloretin was externally applied in the macroscopic experiments and internally in the single channel experiments. However, this is not expected to matter because phloretin is highly lipid soluble. In fact, Strichartz et al. (1980) showed on the squid axon that application from either side produces the same qualitative effects.

The kinetics of the I channels deserve some comment. Jonas et al. (1989) noticed that the closing rate of the I channels is smaller than the deactivation rate of the fast component of the macroscopic tail current. They suggested that the I channels may also contribute to the slow component of the macroscopic tail current. We confirm that the I channels deactivate more slowly than expected from the fast component of the macroscopic tail current. The latter lasts about 20 ms at 12°C and –90 mV (see Fig. 1 of Dubois 1981) whereas I channel openings continue for more than 100 ms at 15°C and –80 mV (Fig. 3). The time constant of the macroscopic fast tail current is about 1 ms at –90 mV and 15°C (see Fig. 6A of Plant 1986), the time constants of the open time histograms in Fig. 7 are 7–9 ms. It seems, however, unlikely to us that the I channels contribute to the slow component of the macroscopic tail current because the latter was never suppressed by phloretin (Kluseman and Meves 1991). We

rather think that the deactivation kinetics of the I channels are different from those of the macroscopic  $I_K$  because the experimental conditions in single channel experiments are entirely different from those on intact nerve fibres.

In contrast to I channels,  $\text{Ca}^{2+}$ -activated maxi K channels of *Xenopus* nerve fibres are activated by phloretin. This has been briefly reported by Klusemann and Koh (1991) and will be more fully described in a future publication.

**Acknowledgement.** We thank the Deutsche Forschungsgemeinschaft for financial support. We are grateful to Professor W. Vogel and D.-S. Koh for showing us the single channel method and to Professor B. Neumcke and Dr. T. D. Plant for reading and discussing a first version of the manuscript.

## References

- Dubois JM (1981) Evidence for the existence of three types of potassium channels in the frog Ranvier node membrane. *J Physiol* 318:297–316
- Fenwick EM, Marty A, Neher E (1982) Sodium and calcium channels in bovine chromaffin cells. *J Physiol* 331:599–635
- Gola M, Ducreux C, Chagneux H (1990)  $\text{Ca}^{2+}$ -activated  $\text{K}^+$  current involvement in neuronal function revealed by in situ single channel analysis in *Helix* neurones. *J Physiol* 420:73–109
- Jonas P, Bräu ME, Hermsteiner M, Vogel W (1989) Single-channel recording in myelinated nerve fibers reveals one type of Na channel but different K channels. *Proc Natl Acad Sci USA* 86:7238–7242
- Jonas P, Koh D-S, Kampe K, Hermsteiner M, Vogel W (1991) ATP-sensitive and Ca-activated potassium channels in vertebrate axons: Novel links between metabolism and excitability. *Pflügers Arch* 418:68–73
- Klusemann J, Koh D-S (1991) Phloretin, a dipolar organic compound, strongly affects the potassium channels of the frog myelinated nerve fibre. 19th Neurobiology Conference Göttingen (abstr) 426
- Klusemann J, Meves H (1991) Phloretin affects the fast potassium channels in frog nerve fibres. *Eur Biophys J* 20:79–86
- Klusemann J, Meves H (1992) The effect of phloretin on single potassium channels of nerve fibres of *Xenopus laevis*. *Pflügers Arch* 420 [Suppl 1]: R32
- Nagy K (1987) Evidence for multiple open states of sodium channels in neuroblastoma cells. *J Membrane Biol* 96:251–262
- Nagy K, Kiss T, Hof D (1983) Single Na channels in mouse neuroblastoma cell membrane. Indications for two open states. *Pflügers Arch* 399:302–308
- Plant TD (1986) The effect of rubidium ions on components of the potassium conductance in the frog node of Ranvier. *J Physiol* 375:81–105
- Spires S, Begenisich T (1989) Pharmacological and kinetic analysis of K channel gating currents. *J Gen Physiol* 93:263–283
- Strichartz GR, Oxford GS, Ramon F (1980) Effects of the dipolar form of phloretin on potassium conductance in squid giant axons. *Biophys J* 31:229–246